Processing of β-BaB$_2$O$_4$ Thin Films Through Metal Organics

TOSHINOBU YOGO, KOICHI KIKUTA AND KAZUO NIWA
Department of Applied Chemistry, School of Engineering, Nagoya University, Furo-cho, Chikusa-ku,
Nagoya 464-01, Japan

MASAO ICHIDA AND ARAO NAKAMURA
Division of Materials Science, Center for Integrated Research in Science and Engineering,
Nagoya University, Furo-cho, Chikusa-ku, Nagoya 464-01, Japan

SHIN-ICHI HIRANO
Department of Applied Chemistry, School of Engineering, Nagoya University, Furo-cho, Chikusa-ku,
Nagoya 464-01, Japan

Abstract. β-BaB$_2$O$_4$ (β-BBO) thin films were successfully synthesized by the sol-gel method using metallo-organic compounds. A stable BBO precursor solution was prepared from barium metal and boron triethoxide or 2,4,6-triethoxycyclotriboroxane in a mixture solvent of ethanol and 2-ethoxyethanol. As-precipitated powder formed by hydrolysis of the precursor solutions crystallized to γ phase, which was transformed to β phase at higher temperatures. The transformation temperatures of powders from γ to β phase of the ethoxide system and the boroxane system were 600 and 680°C, respectively. The calcination of precursor films in a mixture gas of water and oxygen was found to decrease the crystallization temperature of β-BBO films on Pt sheet substrates. The precursor films prepared from the ethoxide system and the boroxane system crystallized to β-BBO on Pt (111)/glass substrates at 500 and 550°C, respectively. The BBO films on Pt(111)/glass substrates showed the strong (006) preferred orientation. The β-BBO films on Pt(111)/glass substrates showed the second harmonic generation (SHG) of the 532 nm light on irradiation with 1064 nm light. The SH power from the BBO films was correlated with the fundamental power through the square-law proportionality based on the theory. The SHG efficiency of the BBO films was dependent upon the film thickness.

Keywords: barium metaborate, metal alkoxide, sol-gel method, thin film, preferred orientation, second harmonic generation

1. Introduction

Barium metaborate (β-BaB$_2$O$_4$, β-BBO) belongs to the space group of R3c with acentric symmetry, and has a layer step type of crystal lattice built up by alternative Ba^{2+} and (B$_3$O$_6$)$^{3-}$ rings [1–3]. The other well-known polymorph of BaB$_2$O$_4$ is α-phase, which belongs to the space group of R$\bar{3}$c having the centric symmetry [4]. The difference between the α (high-temperature) and the β (low-temperature) form is the coordination of the barium by oxygen. On the other hand, γ-BBO is reported to have a chain anion structure similar to Li$_2$B$_2$O$_4$, CaB$_2$O$_4$ and SrB$_2$O$_4$, and no (B$_3$O$_6$)$^{3-}$ rings in the structure [5, 6], although the detailed structure has not been reported yet.

Only β phase is second order nonlinearly active, and is characterized by many remarkable features, such as the large effective second harmonic generation (SHG) coefficients, the wide transparency range, the broad phase-matched region, and the high damage threshold

[7, 8]. β-BBO is one of the useful materials for the phase matching in the ultraviolet frequency region. The flux method and the Czochralski method have been used for the growth of β-BaB$_2$O$_4$ single crystals [9–11]. The structure of melt is closely related to the nucleation of β-BaB$_2$O$_4$ from melt, and reflects the structure and crystallinity of starting powders [11]. Recently, the preparation of oriented thin films of β-BaB$_2$O$_4$ has been receiving great attention because of its applications in integrated non-linear optical devices.

The sol-gel process has many advantages, such as high purity of product, low processing temperature, precise composition control, and the formation of epitaxial coating films. Low temperature crystallization and highly preferred orientation of alkoxy-derived niobate and titanate thin films can be promoted by controlling the structure of double alkoxides in solution [12] and the crystallization atmosphere of gel films as well as the crystallographic plane of the substrate [13–15]. Highly oriented LiNbO$_3$ film can be crystallized as low as 250°C using a H$_2$O-O$_2$ gas flow during calcination under the controlled crystallization conditions [13]. Water vapor during calcination plays a prominent role for the crystallization into the perovskite phase of Pb(Zr,Ti)O$_3$ [16], K(Ta,Nb)O$_3$ [17] and Pb(Mg,Nb)O$_3$-PbTiO$_3$ films [18] without any pyrochlore phases, which degrade ferroelectric properties.

Hirano et al., synthesized β-BaB$_2$O$_4$ powders and films using boron ethoxide and barium alkoxide [19, 20]. This paper describes the synthesis of highly oriented β-BaB$_2$O$_4$ films on Pt sheet substrates and Pt(111)/glass substrates from two kinds of starting boron compounds, boron ethoxide and 2,4,6-triethoxycyclotriboroxane. 2,4,6-triethoxycyclotriboroxane consists of a six-member ring of alternating borons and oxygens, which is included in the structure of BaB$_2$O$_4$. Crystallization of β-BaB$_2$O$_4$ thin films were dependent strongly upon the precursor structure and calcining conditions. The calcination of precursor films in a gas mixture or water and oxygen was found to be effective for low temperature synthesis of highly oriented crystalline β-BaB$_2$O$_4$ films. β-BaB$_2$O$_4$ thin films with preferred orientation were successfully synthesized on Pt(111)/glass substrates from metal alkoxides. The *c*-axis oriented β-BaB$_2$O$_4$ films exhibited the frequency doubling of Nd:YAG laser light.

2. Experimental Procedure

Ethanol was dried over magnesium ethoxide and distilled before use. 2-Ethoxyethanol (Ethylene glycol
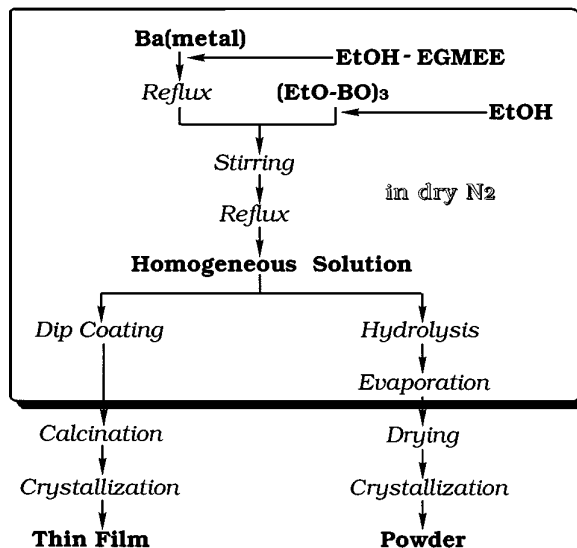

Figure 1.   Scheme for processing of alkoxy-derived BBO powders and films using 2,4,6-triethoxycyclotriboroxane.

monoethyl ether, EGMEE) was dried with molecular sieve and distilled before use. Barium metal and boron triethoxide were commercially available. 2,4,6-Triethoxycyclotriboroxane, (B(OEt)-O)$_3$, was prepared according to the literature [21]. Figure 1 illustrates the experimental procedure for preparing BBO powder and thin film from barium metal and 2,4,6-triethoxycyclotriboroxane. All procedures were carried out in a dry nitrogen atmosphere. The precursor solution synthesized from barium metal and boron ethoxide or 2,4,6-triethoxycyclotriboroxane in absolute ethanol was slightly unstable and inhomogeneous. As an additive, 2-ethoxyethanol (EGMEE) was found to yield a homogeneous precursor solution for BBO. Ba metal chips were added by portions to a mixture solution of ethanol and EGMEE and refluxed producing a barium alkoxide solution. 2,4,6-Triethoxycyclotriboroxane dissolved in ethanol was added to the solution. The mixed solution was reacted by refluxing for 20 h to yield a clear and homogeneous solution. The solution (boroxane system) was condensed to about 0.1 mol/l by removal of solvents at around 80°C, which had appropriate properties for the film preparation by dip coating. Similarly, a precursor solution (ethoxide system) was prepared from barium metal and boron triethoxide.

The solution was hydrolyzed with excess water, and the solvent was evaporated yielding powders. The powders were then heat-treated at temperatures from 350 to 1000°C for 1 h at a heating rate of 10°C/min.
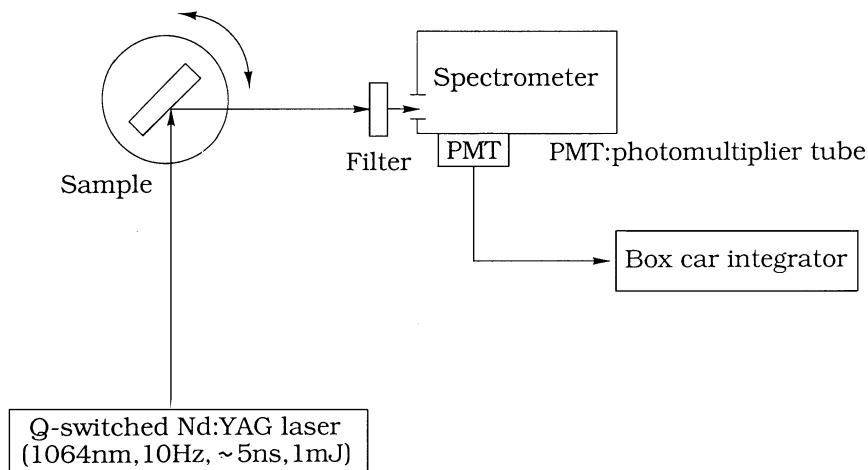
Figure 2. Experimental setup for the SHG measurement of β-BBO films on Pt(111)/glass substrates.

Films were fabricated using the precursor solution by dip coating on Pt sheet substrates and Pt(111)/glass substrates. Pt layers were deposited on glass plates (Corning 7059) by RF magnetron sputtering. The dip coating on substrates was carried out by dipping a substrate in the precursor solution and withdrawing at a fixed speed of 1.5 mm/sec followed by drying in dry N$_2$ for several minutes. The precursor films were calcined at 350°C for 1 h in a gas mixture of water and oxygen. The oxygen gas bubbled through water kept at 54°C (P$_{H_2O}$, 112 mmHg) was introduced to the furnace. The calcined films were placed into a preheated furnace at a desired temperature and heat-treated at the temperature for 1 h in flowing dry oxygen. This procedure was repeated several times to increase the film thickness. The crystallized film thickness per dip coating was about 0.05 μm.

Carbon-13 nuclear magnetic resonance (^{13}C NMR) spectra were measured in CDCl$_3$ using tetramethylsilane (TMS) as the reference of chemical shift. Infra red (IR) spectra were measured by the KBr method using a Nicolet 5DXB spectrometer.

The burn-out and crystallization behaviors of powders were analyzed by differential thermal analysis (DTA)-thermogravimetry (TG) at 10°C/min. Prepared powders and crystallized films were characterized by X-ray diffraction analysis (XRD) using CuKα radiation with a monochromator and by scanning electron microscopy (SEM). The powders were also analyzed by transmission electron microscopy (TEM). The BBO films on Pt(111)/substrates were exposed to 1064 nm light from Nd^{3+}:YAG laser with the pulse duration of 5 ns to investigate the second harmonic generation

(SHG) effect. The peak power of laser light irradiated on the films was 200 kW. The reflected light from the specimen was analyzed by a spectrometer with a photomultiplier and a box car integrator as shown in Fig. 2.

3. Results and Discussion

3.1. Characterization of BBO Precursor

Figure 3 shows ^{13}C NMR spectra of BBO precursors formed from B(OC$_2$H$_5$)$_3$ and (B(OEt)-O)$_3$. The chemical shifts of 2-ethoxyethoxy group of BBO precursors shown in Fig. 3 are as follows: BBO precursor from (B(OEt)$_3$ (Fig. 3(a)); 72.5 ppm (O$\underline{C}$H$_2$CH$_2$ OCH$_2$CH$_3$), 66.5 ppm (OCH$_2$$\underline{C}H_2OCH_2CH_3$), 60.6 ppm (OCH$_2CH_2O\underline{C}H_2CH_3$) and 15.2 ppm (OCH$_2$ CH$_2$OCH$_2$$\underline{C}H_3$), BBO precursor from (B(OEt)O)$_3$ (Fig. 3(b)); 72.2 ppm, 66.3 ppm, 60.1 ppm and 14.9 ppm. The ethoxy group of starting B(OC$_2$H$_5$)$_3$ appears at 59.1 ppm (O$\underline{C}$H$_2$) and 17.3 ppm (OCH$_2$$\underline{C}H_3$). (B(OEt)-O)$_3$ shows the signals of ethoxy groups at 60.0 ppm and 17.0 ppm. Although free ethoxyethanol (EGMEE) is observed in the spectra (Fig. 3(b)) [22], the signals of ethoxy group of starting alkoxides disappear by the reaction with barium in ethanol-ethoxyethanol. The ethoxy groups of starting B(OEt)$_3$ and (B(OEt)O)$_3$ are substituted for 2-ethoxyethoxy (OCH$_2$CH$_2$OCH$_2$CH$_3$) groups. The difference of chemical shifts of ethoxyethoxy group in each BBO precursor reveals the formation of different precursors, which originate from the different backbone structures [23].
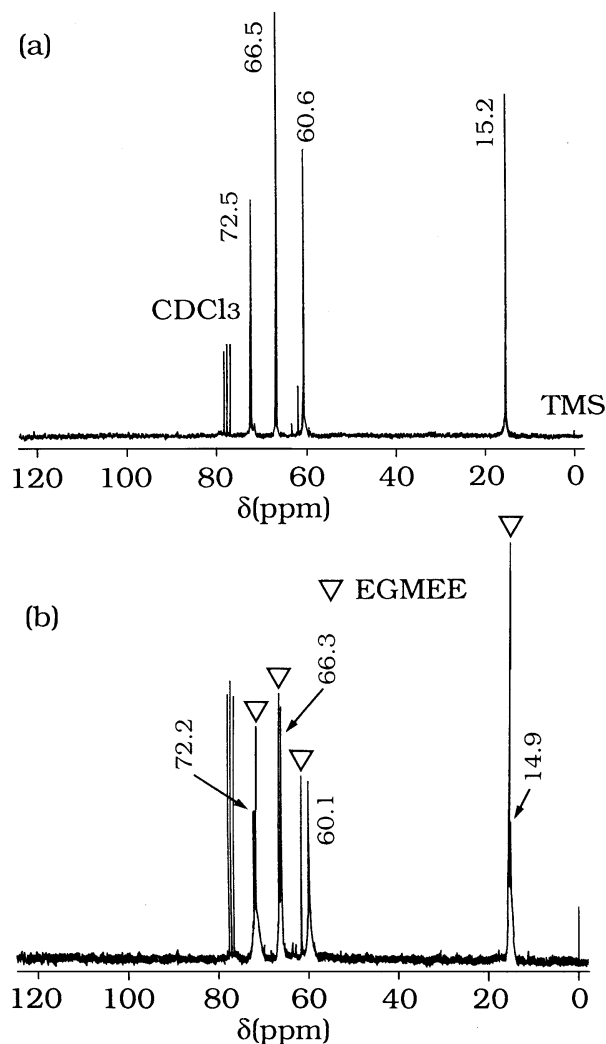
(a)

(b)

Figure 3. ^{13}C NMR spectra of BBO precursor prepared from (a) B(OC$_2$H$_5$)$_3$ and (b) 2,4,6-triethoxycyclotriboroxane.

3.2. Crystallization of Alkoxy-Derived Powders

The precursor solution of alkoxides was hydrolyzed with an excess amount of water for complete precipitation. Figure 4 shows the DTA-TG curve of the powder formed from the boroxane system from room temperature to 1000°C at a heating rate of 10°C/min. On heating, the TG curve shows a weight loss below 150°C due to the evaporation of low boiling components including water and alcohol. Large exothermic peaks from 200 to 450°C are attributable to the burning of organic moieties.

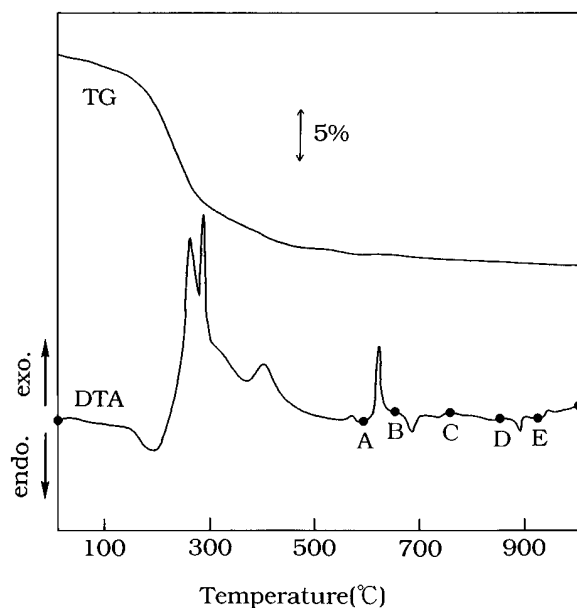The products from the boroxane system were analyzed by XRD after quenched from various

Figure 4. DTA-TG curves of BBO powders formed from the boroxane system. A; 580°C, B; 640°C, C; 750°C, D; 830°C, E; 925°C.

temperatures during DTA-TG measurement. After most organics were removed, γ phase of low crystallinity was observed at 580°C (point A). Although γ phase remained at 640°C (point B), the crystallinity of β phase increased markedly. Thus, the exotherm at 620°C is attributed to the crystallization of γ phase. β phase was observed at 750°C (point C), which was just after an endothermic peak at 680°C. The small endotherm at 680°C, therefore, corresponds to the transformation of γ phase to β phase on heating at 10°C/min. β phase was observed at 830°C (point D). Since α phase was confirmed at 925°C (point E), an endothermic peak at 880°C is derived from the transformation of β to α phase. Based upon a similar quench experiment, the powder from the ethoxide system was found to crystallize to β-BBO at 600°C [20]. The formation temperature of β-BBO in the ethoxide system was lower by 80°C than that of the boroxane system.

Figure 5 shows the IR spectra of powders heat-treated in H$_2$O-O$_2$ flow for 4 h followed by the heat treatment in O$_2$ flow for 4 h at 450°C. The OH absorption remains at 3400 cm^{-1} in the both spectra due to the water vapor treatment. The CH absorptions at 2900 cm^{-1} disappear by the treatment. The absorptions at 1400, 990, 746 and 569 cm^{-1} in the ethoxide-derived powder shown in Fig. 5(a) are assigned to the characteristic band of chain-type γ phase [5, 24]. The bands at
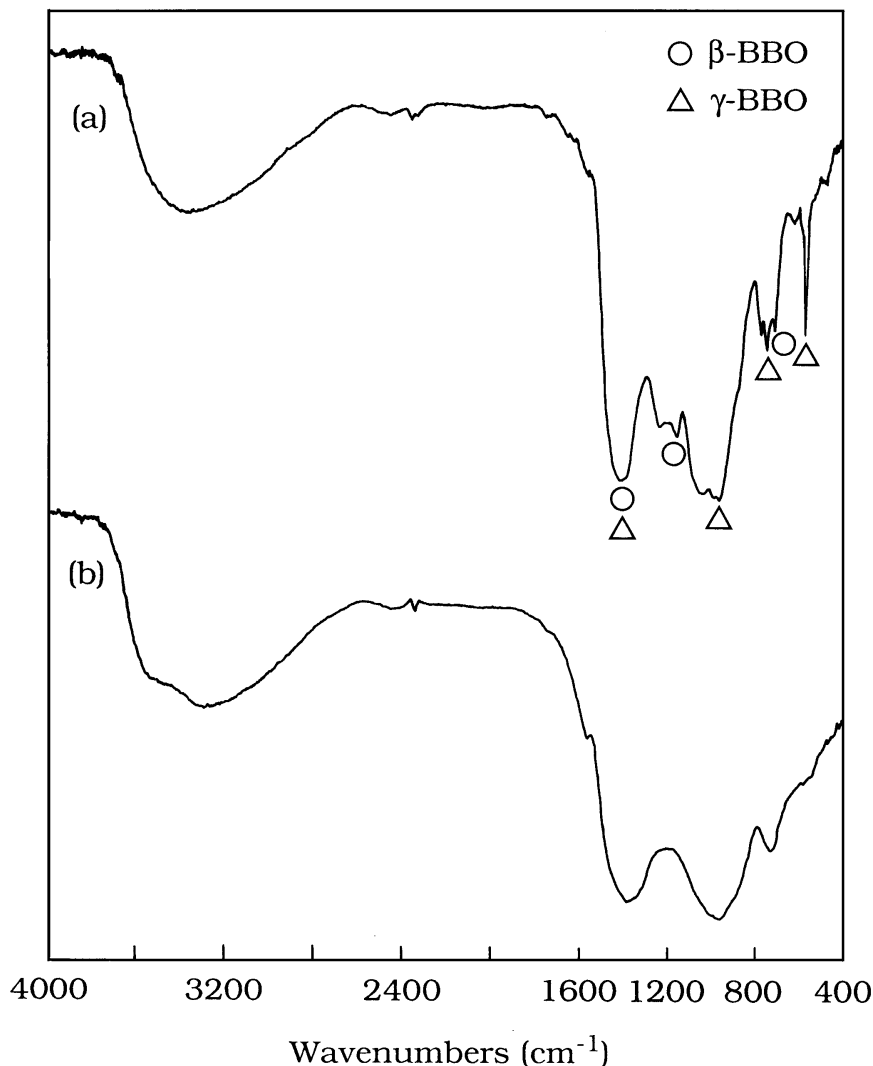
Figure 5. IR spectra of powders heat-treated at 450°C from ethoxide system and boroxane system. (a) ethoxide system, (b) boroxane system.

1400, 1180 and 711 cm^{-1} are ascribed to β-BBO. The specimen shown in Fig. 5(a) consists of β and γ phases. On heating the powder above 450°C, the absorption at 1180 cm^{-1} increased in intensity with decreasing intensities of the absorptions at 990, 746 and 569 cm^{-1}. This change corresponds to the transformation of γ to β phase. In the boroxane system, however, the bands are broad, and no distinct absorptions of β and γ phase are observed as shown in Fig. 5(b). At 450°C, the product from the boroxane system is amorphous solid including (B—O)$_n$ bonds. This result reveals the feasible formation of borate phase in the ethoxide system below 450°C.

The powders were also analyzed by TEM. The selected area diffraction (SAD) of the powder from the ethoxide system at 450°C exhibits several rings consisting of spots (Fig. 6(a)). However, the SAD of the powder from the boroxane system comprises hallo rings as shown in Fig. 6(b). The diffraction pattern of Fig. 6(a) is in good agreement with those of BBO, although β phase is not distinguished from the γ phase. The result also indicates the facile formation of BBO crystallite in the ethoxide system at lower temperature.

Figures 7 and 8 show XRD profiles of powders prepared from the ethoxide system and the boroxane system, respectively, after heat treatment above 500°C
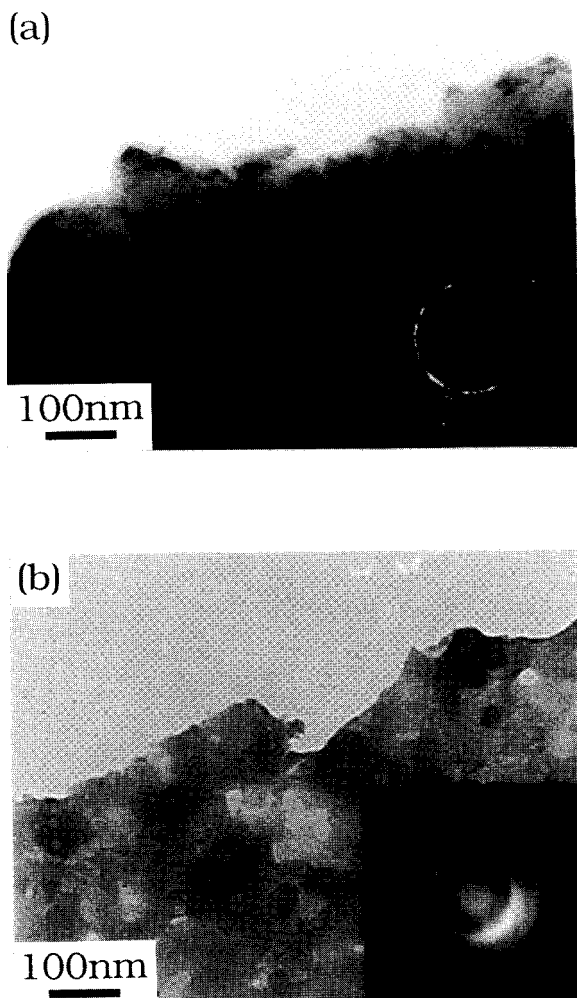
(a)

100nm

(b)

100nm

Figure 6. Microstructures and selected area diffractions of powders (a) powder from the ethoxide at 450°C, (b) powder from the boroxane system at 500°C.
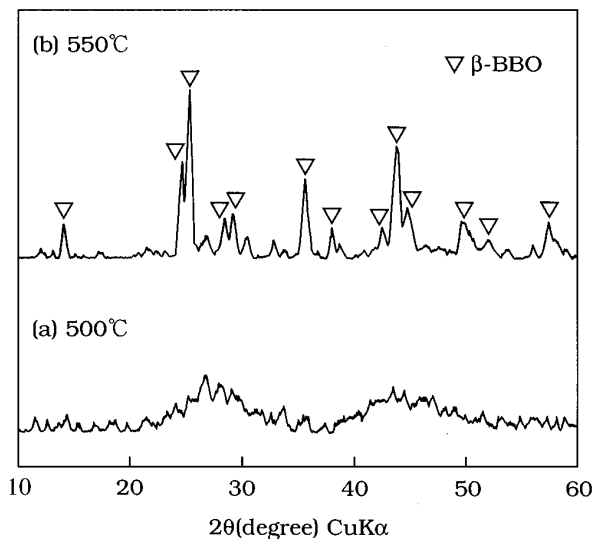

Figure 7. XRD profiles of BBO powders synthesized from the ethoxide system crystallized at 500 and 550°C for 1 h. (a) 500°C, (b) 550°C.
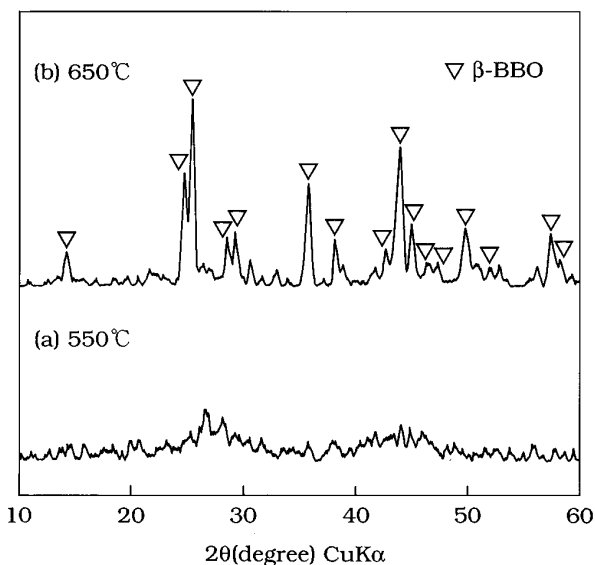

Figure 8. XRD profiles of BBO powders prepared from the boroxane system crystallized at 550 and 650°C for 1 h. (a) 550°C, (b) 650°C.

for 1 h. The ethoxide-derived powder is X-ray amorphous at 500°C (Fig. 7(a)), and crystallizes to β-BBO at 550°C for the duration time of 1 h as shown in Fig. 7(b). However, the powder from the boroxane system heat-treated at 550°C has low crystallinity without any sharp reflections (Fig. 8(a)). Crystalline β-BBO phase is obtained from the boroxane-derived powder after heat treatment at 650°C for 1 h as shown in Fig. 8(b).

The formation of γ phase in the both systems supports that the chain-type borate is formed from amorphous powder before the formation of $(B_3O_6)^{3-}$ ring of β-BBO. β phase crystallized in the ethoxide system at lower temperatures compared with in the boroxane system. The bond scission of the boroxane ring

of starting compound gives a ring-opened chain structure, which again yields $(B_3O_6)^{3-}$ ring structure in the β-BBO. Similar to borazine, $(BHNH)_3$, there is probably π bonding character in the boroxane ring, which is more stabilized by delocalization of π electrons than the B—O bonds of boron alkoxide. As the boroxane ring is cleaved during heating, the more energy

is required for the formation of γ phase than that from the ethoxide-derived precursor. Accordingly, the chain of γ phase was formed at higher temperatures in the boroxane system. Above 600°C, the $(B_3O_6)^{3-}$ ring was formed again as a constituent of the BBO crystal lattice. On the other hand, the ethoxide-derived precursor directly produces γ phase, which was transformed to β phase below 600°C.

3.3. Formation of BBO Thin Films on Pt(111)/Glass Substrates

Since the β-BBO films on Pt(111)/glass substrates have a better orientation than those on Pt sheet substrates, Pt(111)/glass was employed as a substrate [20]. Figure 9 shows XRD profiles of 1.0 μm-thick films on Pt(111)/glass substrates from the ethoxide system and the boroxane system after heat treatments at 500 and 550°C. The precursor films were calcined at 350°C for 1 h in a gas mixture of water/oxygen. The precursor films formed from the ethoxide system crystallize to β phase at 500°C as shown in Fig. 9(a). The
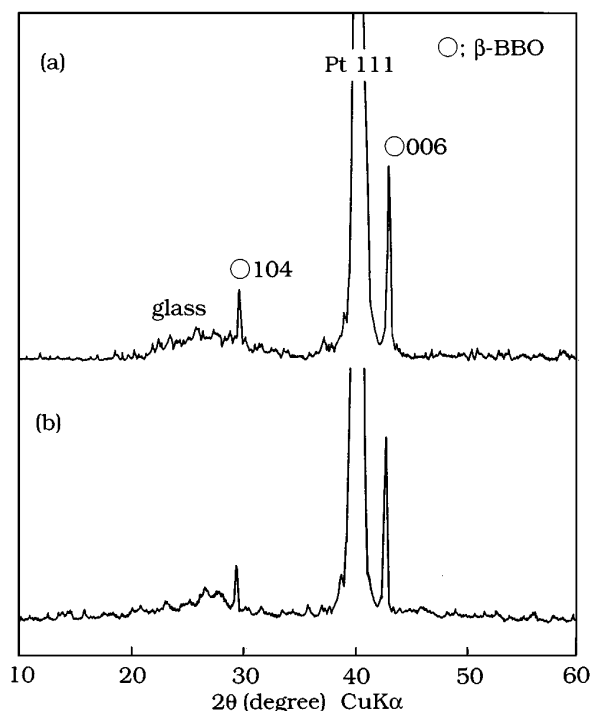

Figure 9. XRD profiles of BBO thin films on Pt(111)/glass substrates calcined at 350°C for 1 h in H$_2$O/O$_2$ flow, and then crystallized at 500 and 550°C 1 h in O$_2$ flow. (a) ethoxide system, 500°C, (b) boroxane system, 550°C.

film from the boroxane system gives a X-ray amorphous film at 500°C, which crystallizes to β phase at 550°C (Fig. 9(b)). The BBO films synthesized from the both systems show a (006) preferred orientation on Pt(111)/glass substrates, since 113 reflection has the maximum intensity for β-BBO powders.

The characteristic $(B_3O_6)^{3-}$ ring of β phase is formed at about 600°C, when the precipitated powder from the ethoxide system is heated. On the other hand, the precursor films on Pt(111)/glass crystallize to β phase at 500°C which is lower than that for powders. The hydrolyzed powder from the boroxane system crystallize to β-BBO at 670°C. However, the β-BBO film crystallizes on Pt(111)/glass substrates at 550°C. The feasible formation of β-BBO phase in film is attributed to the assistance of nucleation sites with atomic alignment of substrates.

The anion $(B_3O_6)^{3-}$ group in β-BBO is nearly planar with its plane perpendicular to the threefold axis which passes through the center of the ring. The planar ring anion $(B_3O_6)^{3-}$ has a threefold symmetry, and is parallel to (006) plane of the unit cell of β-BBO. The Pt(111) plane of Pt is the most close-packed plane, and has a threefold axis, which matches that of the $(B_3O_6)^{3-}$ ring parallel to (006). Thus, the (006) orientation is generally observed on Pt(111)/glass substrates. On the other hand, the interaction between $(B_3O_6)^{3-}$ rings and Ba^{2+} ions is considered to be strong for the (104) plane direction in the unit cell [1]. Therefore, the (104) plane is also easily developed during crystallization.

Edge-on SEM photomicrographs of BBO films on Pt(111)/glass substrates from the ethoxide system and the boroxane system are shown in Fig. 10. The film from the ethoxide system (Fig. 10(a)) comprises a smooth surface with no cracks and voids, and is superior in film quality to the film from the boroxane system (Fig. 10(b)).

3.4. Second Harmonic Generation (SHG) of BBO Thin Films

The SHG effect was analyzed for β-BBO thin films on Pt(111)/glass substrates synthesized from the ethoxide system at 550°C. The films were exposed to incident light of 1064 nm from a Nd:YAG laser. The reflected light from β-BBO film was found to include 532 nm light. Figure 11 shows the relations between the powers of incident light and of reflected light (SH wave) from β-BBO films on Pt(111)/glass substrates. The slopes of curves of 0.4 μm and 1.0 μm thick-films
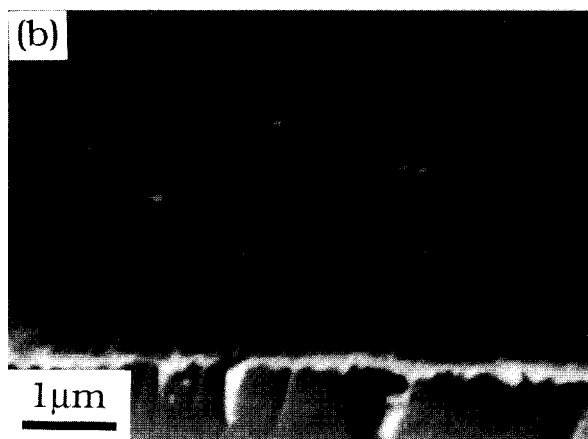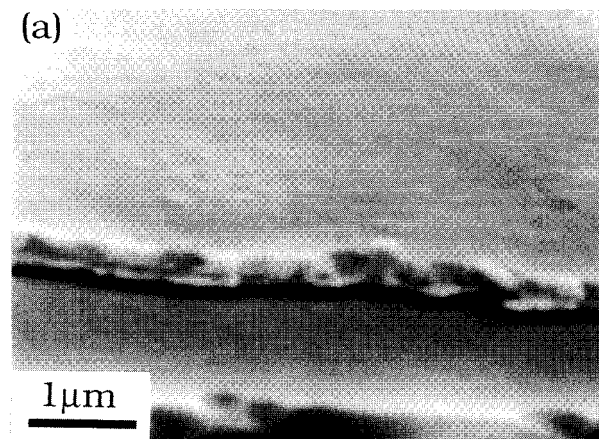
(a)

1μm

(b)

1μm

Figure 10. Edge-on SEM photographs of fractured BBO films crystallized at 550°C for 1 h on Pt(111)/glass substrates. (a) ethoxide system, (b) boroxane system.

Figure 11. The relation of power between fundamental light (1064 nm) and second harmonic light (532 nm) for β-BBO thin films on Pt(111)/glass substrates crystallized at 550°C. (a) film thickness: 0.4 μm, (b) film thickness: 1.0 μm.

the longer interaction length between the film and the light.

4. Conclusions

Crystalline β-BBO films with highly preferred orientation were successfully synthesized on Pt(111)/glass substrates from metallorganics. The results are summarized as follows:

1. A homogeneous and stable precursor solution was prepared from boron ethoxide or 2,4,6-triethoxycyclotriboroxane, barium metal, with an ethoxyethanol in ethanol additive.
2. The hydrolyzed powder from the ethoxide system crystallized to β phase at 600°C, which was lower by 80°C than that from the boroxane system. The ethoxide system was found to be more promising than the boroxane system for the low temperature synthesis of β-BBO.
3. Water vapor during calcination of gel films was found to have a pronounced effect on the low temperature crystallization of β-BBO.
4. β-BBO films with c-axis preferred orientation were synthesized from the ethoxide system and boroxane system at 500 and 550°C, respectively, on Pt(111)/glass substrates.

are 1.90 and 2.06, respectively, which are almost equal to 2. Therefore, both lines satisfy the square-law proportionality between the fundamental power (P_ω) and the harmonic power ($P_{2\omega}$). The SH power from the thick film (1.0 μm) is larger than that from the thin film (0.4 μm) as shown in Fig. 11. The SHG efficiency from the power relation increases from 10^{-12} to 10^{-10} with increasing film thickness from 0.4 to 1.0 μm. The phase-matched efficiency of β-BBO crystal (4 mm thickness) is usually $10^{-2} \sim 10^{-1}$. The film thickness is sufficiently small compared to the coherence length of bulk BBO ($l_c = 15$ μm) [7]. The efficiency of the current film is smaller than that of the single crystal, since the phase match condition is not satisfied. The better efficiency of the 1.0 μm-thick film results from
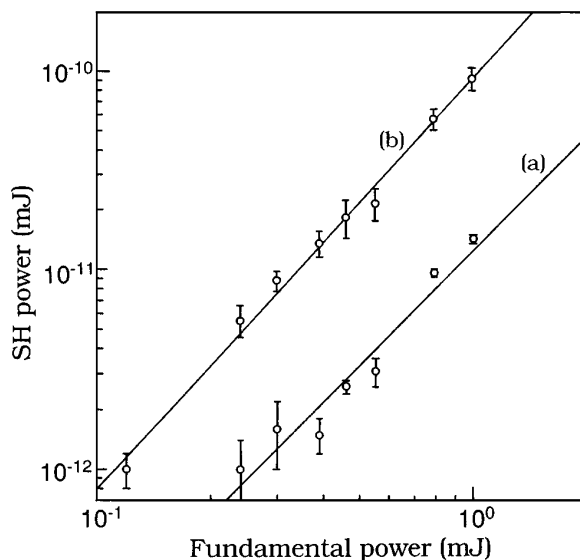
5. The (006)-oriented β-BBO films on Pt(111)/glass substrates crystallized at 550°C were confirmed as a generator of the second harmonic wave. The SHG efficiency increased with increasing film thickness.

Acknowledgment

References

1. S. Lu, M. Ho, and J. Jiang, Acta. Phys. Sinica. **31**, 948 (1982).
2. J. Liebertz and S. Stähr, Z. Kristallogr. **165**, 91 (1983).
3. R. Frönlich, Z. Kristallogr. **168**, 109 (1984).
4. A.D. Mighell, A. Perloff, and S. Block, Acta. Cryst. **20**, 819 (1969).
5. O. Yamaguchi, K. Tominaga, and K. Shimizu, Ceramurgia Intl. **6**, 103 (1980).
6. JCPDS Cards, 35–181.
7. C.T. Chen, B.C. Wu, A.D. Jiang, and G.M. You, Sci. Sin. Ser. B (Eng. Ed.) **28**, 235 (1985).
8. D. Eimerl, L. Davis, S. Velsko, E.K. Graham, and A. Zalkin, J. Appl. Phys. **62**, 1968 (1987).
9. L.K. Cheng, W. Bosenberg, and V.L. Tang, J. Cryst. Growth **89**, 553 (1988).
10. R.S. Feigelson, R.J. Raymeker, and R.K. Route, J. Cryst. Growth **97**, 352 (1989).
11. K. Itoh, F. Marumo, and Y. Kuwano, J. Cryst. Growth **106**, 728 (1990).
12. S. Hirano and K. Kato, Adv. Ceram. Mater. **2**, 142 (1987).
13. S. Hirano and K. Kato, Adv. Ceram. Mater. **3**, 503 (1988).
14. S. Hirano and K. Kato, J. Non-Cryst. Solid **100**, 538 (1988).
15. S. Hirano, K. Kikuta, and K. Kato, Mat. Res. Soc. Symp. Proc. **200**, 3 (1990).
16. S. Hirano, T. Yogo, K. Kikuta, Y. Araki, M. Saito, and S. Ogasahara, J. Amer. Ceram. Soc. **75**, 2785 (1992).
17. S. Hirano, T. Yogo, K. Kikuta, T. Morishita, and Y. Ito, J. Amer. Ceram. Soc. **75**, 1701 (1992).
18. S. Hirano, T. Yogo, K. Kikuta, K. Kato, W. Sakamoto, and S. Ogasahara, *Ceram. Trans., Ferroelectric Films*, edited by A.S. Bhalla and K.M. Nair (Amer. Ceram. Soc., Westerville, OH, 1992), vol. 25, pp. 19–32.
19. S. Hirano, T. Yogo, K. Kikuta, and K. Yamagiwa, J. Amer Ceram. Soc. **75**, 2590 (1992).
20. S. Hirano, T. Yogo, K. Kikuta, K. Yamagiwa, and K. Niwa, J. Non-Cryst. Solid. **178**, 293 (1994).
21. M.F. Lappert, J. Chem Soc. 2790 (1958).
22. J. Pouchert and J. Behnke, *The Aldrich Library of ^{13}C and ^1H FT-NMR Spectra* (Aldrich Chemical, Milwaukee, WI, 1992).
23. E. Breitmaier and W. Voelter, *Carbon-13 NMR Spectroscopy* (VCH, New York, 1987).
24. C.E. Weir and R.A. Schroeder, J. Res. Natl. Bur. Stand. **68A**, 465 (1964).